JOBNAME: JGS PAGE: 1 SESS: 32 OUTPUT: Wed Sep 26 15:06:45 2001
/hling/journals/geo/195/00139

Journal of the Geological Society, London, Vol. **158**, 2001, pp. 855–867. Printed in Great Britain.

The role of crustal and mantle sources in the genesis of granitoids of the Antarctic Peninsula and adjacent crustal blocks

I. L. MILLAR[1], R. C. R. WILLAN[2], C. D. WAREHAM[2] & A. J. BOYCE[3]

[1]*British Antarctic Survey, c/o NERC Isotope Geosciences Laboratory, Keyworth, Nottingham NG12 5GG, UK (e-mail: ilm@bas.ac.uk)*

[2]*British Antarctic Survey, High Cross, Madingley Road, Cambridge CB3 0ET, UK*

[3]*Isotope Geoscience Unit, Scottish Universities Environmental Research Centre, East Kilbride, Glasgow G75 0QF, UK*

Abstract: Magmatic rocks from the Antarctic Peninsula show marked variations in isotope composition, which reflect changes in the geodynamic evolution of the peninsula through time. Most Antarctic Peninsula granitoids formed as a result of subduction: they fall on well-defined trends on plots of εNd, $^{207}Pb/^{204}Pb$ and $\delta^{18}O$ against $^{87}Sr/^{86}Sr_i$, between a component derived from subduction-modified mantle or juvenile basaltic underplate (εNd_i>6, $^{207}Pb/^{204}Pb$=15.61, $\delta^{18}O$=5.5‰, $^{87}Sr/^{86}Sr$<0.704) and an end-member interpreted as a melt of Proterozoic lower crust (εNd=–7, $^{207}Pb/^{204}Pb$=15.67, $\delta^{18}O$=10‰, $^{87}Sr/^{86}Sr$=0.709). A small group of granitoids, emplaced before or during Gondwana break-up, plot on distinct trends towards high $^{87}Sr/^{86}Sr_i$ compositions, reflecting mixing between melts derived from Proterozoic lower crust and melts of middle–upper crustal rocks (εNd_i=–9, $^{207}Pb/^{204}Pb$=15.64, $\delta^{18}O$=10‰, $^{87}Sr/^{86}Sr$=0.726), with little or no input of new material derived from the mantle or from juvenile basaltic underplate. These granitoids are thought to have formed as a result of crustal attenuation during the initial rifting phase of Gondwana break-up. Similar trends are shown by data from granitoids of the adjacent crustal blocks of West Antarctica. The isotope data suggest that an enriched Ferrar/Karoo-type lithosphere was not involved in the genesis of granitoids of the Antarctic Peninsula or of the Ellsworth–Whitmore Mountains crustal block.

Keywords: Antarctica, Gondwana, granites, isotopes, subduction.

Magmatic rocks generated at continental destructive plate margins may contain components derived from melts of the subducting slab, subducted sediments, continental crust, including melts of mafic underplate at the base of the crust, and the sub-continental lithospheric and asthenospheric mantle (e.g. Hildreth & Moorbath 1988; Rogers & Hawkesworth 1989; Defant & Drummond 1990; Atherton & Petford 1993; Pankhurst *et al.* 1999). In many subduction-related magmatic suites, the importance of melting at middle to upper crustal levels can be deduced from systematic variations in Sr, Nd and O isotope signatures (James 1981). Mixing between high-εNd_i, low-$^{87}Sr/^{86}Sr_i$ mafic arc magmas and melts of relatively old, low-εNd_i, high $^{87}Sr/^{86}Sr_i$ crust gives rise to concave-upwards hyperbolic arrays on plots of εNd_i against $^{87}Sr/^{86}Sr_i$. In contrast, steep linear arrays on plots of εNd_i against $^{87}Sr/^{86}Sr_i$ have been attributed to melting and assimilation processes in the lower crust (Hildreth & Moorbath 1988; Pankhurst *et al.* 1999) or to the mobilization of ancient lithospheric mantle (Rogers & Hawkesworth 1989).

The plutonic and associated hypabyssal igneous rocks that make up the Antarctic Peninsula magmatic arc (Figs 1 & 2) range in composition from metaluminous I-type granites, tonalities and gabbros, through to peraluminous granites. Given the broad range in composition and emplacement environment of these rocks, they will be referred to collectively here as 'granitoids'. Previous studies have suggested that the Antarctic Peninsula granitoids fall on simple, concave-upwards hyperbolae on plots of εNd_i against $^{87}Sr/^{86}Sr_i$, and have explained these trends by invoking mixing of mafic arc magmas with melts of high-$^{87}Sr/^{86}Sr_i$–low εNd_i crustal rocks (e.g. Pankhurst *et al.* 1988; Hole *et al.* 1991; Wever *et al.* 1994; Wareham *et al.* 1997*a, b*). In this paper we re-evaluate the existing isotope data for Antarctic Peninsula granitoids, and present new Sr, Nd and Pb isotope data in order to test these mixing models. Our data indicate that melting of high-$^{87}Sr/^{86}Sr$ middle–upper crust was *not* an important process in the formation of most Antarctic Peninsula granitoids. Rather, the composition of most granitoids is controlled by melting and assimilation processes in the lower crust. Extensive crustal melting was restricted to Late Triassic to Mid-Jurassic times, and may reflect extension associated with the initial rifting phase of Gondwana break-up. Comparison with granitoids of the adjacent Ellsworth–Whitmore Mountains and Thurston Island crustal blocks (Fig. 1) suggests that melting of both lower and upper crust was widespread throughout the region in Triassic to Mid–Jurassic times.

Geological setting

The Antarctic Peninsula magmatic arc is built, at least in part, on continental crust with a record of magmatism and metamorphism that stretches back at least to Cambrian times, although pre-Mesozoic basement rocks are only sparsely exposed. Orthogneisses with protolith ages of *c.* 450–550 Ma crop out in small areas of eastern Graham Land and NW Palmer Land (Millar *et al.* in press). Paragneisses that form the basement to Triassic granites and granodiorites in eastern Palmer Land are no older than Late Cambrian, but show patterns of zircon inheritance typical of derivation from a

JOBNAME: JGS PAGE: 2 SESS: 33 OUTPUT: Wed Sep 26 15:06:45 2001
/hling/journals/geo/195/00139

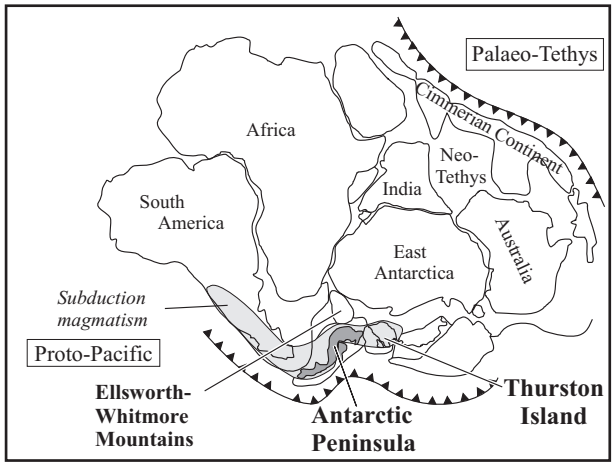

Fig. 1. Map of Gondwana, showing proposed location of pre-break-up subduction zone along the Proto-Pacific margin.

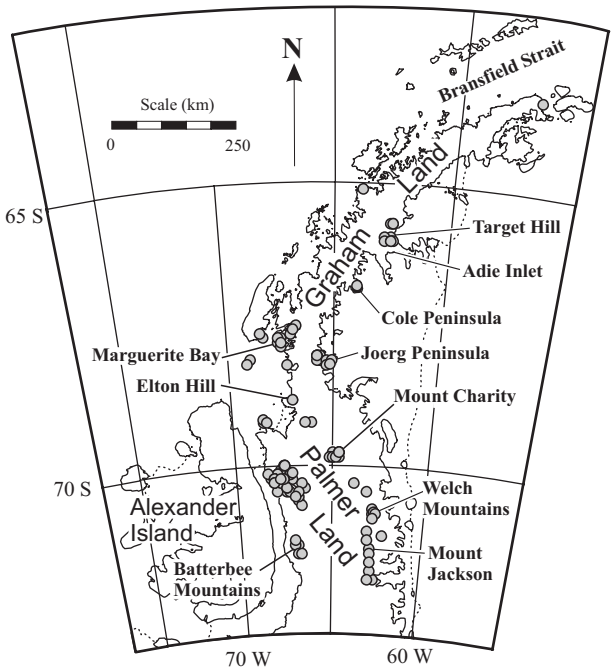

Fig. 2. Map of the Antarctic Peninsula, showing the distribution of granitoids analysed in this study, and highlighting key localities.

source within Gondwana (Millar *et al.* in press). A few small granite bodies were intruded in eastern Graham Land at *c.* 400 Ma (Milne & Millar 1989): such granites have been identified elsewhere in the peninsula as clasts within conglomerates (Pankhurst 1983; Loske & Miller 1991; Tangeman *et al.* 1996). Locally, the basement underwent metamorphism, migmatization and granite emplacement during Carboniferous (*c.* 325 Ma) and Permian (*c.* 260 Ma) times.

The plutonic rocks which form the Antarctic Peninsula batholith were emplaced between *c.* 240 Ma and 10 Ma (Leat *et al.* 1995), a period which spans the Jurassic break-up of Gondwana and subsequent segmentation of West Antarctica. They intrude basement gneiss, volcanic rocks of the arc, back-arc sedimentary rocks, and sedimentary rocks in a fore-arc accretionary complex.

Triassic and Early Jurassic plutons were emplaced along the palaeo-Pacific margin of Gondwana, prior to the break-up of the supercontinent (Fig. 1). Granitoid emplacement and migmatization of basement gneisses were widespread in northern Palmer Land at this time (*c.* 230–200 Ma). The earliest plutons are peraluminous granites, with S-type characteristics and relatively high $^{87}Sr/^{86}Sr_i$, and formed largely by melting of local paragneissic basement (Wever *et al.* 1994). By 205 Ma, metaluminous, I-type granodiorites were also being generated. It is possible that this magmatism represented the initiation of subduction along the Gondwana margin (e.g. Pankhurst 1982; Leat *et al.* 1995).

Magmatism associated with the Jurassic break-up of Gondwana is represented by extensive silicic volcanism and associated subvolcanic plutonism, contemporaneous with eruption of the Jurassic ignimbrites of Patagonia. Zircon U–Pb ages from this extensive volcanic province show that magmatism migrated away from the continental interior, where it began at *c.* 185 Ma, and reached the western margin of the Peninsula by 155 Ma (Pankhurst *et al.* 1999). In the adjacent Ellsworth–Whitmore Mountains crustal block (Fig. 1), granites associated with the break-up of Gondwana have within-plate characteristics (Storey *et al.* 1988) and may contain components derived from an enriched lithospheric mantle source, and melts of continental crust.

Cretaceous and younger plutons were emplaced as a result of east-directed subduction of proto-Pacific oceanic crust beneath the Antarctic Peninsula (Suarez, 1976; Saunders *et al.* 1980; Pankhurst 1982; Storey *et al.* 1992). These range in composition from gabbro to granodiorite and are dominated by metaluminous, calcic, Si-oversaturated compositions. Unequivocal subduction-related plutonism was initiated by *c.* 140 Ma, and was most voluminous and widespread between 125 and 100 Ma. The Tertiary part of the batholith is restricted to the west coast of the northern Antarctic Peninsula, signifying a major westwards jump in the locus of the arc. Subduction and its associated magmatism ceased in the Antarctic Peninsula between *c.* 50 Ma and the present-day, following a series of northward-younging ridge–trench collisions (Barker 1982; Larter & Barker 1991).

Granitoid components

The geochemical and isotopic characteristics of Antarctic Peninsula granitoids have been explained in terms of mixing of a variety of magmas derived from the mantle, or from juvenile basaltic lower crust, with melts of middle or upper crustal rocks (e.g. Pankhurst 1982; Hole 1986; Pankhurst *et al.* 1988; Hole *et al.* 1991; Wever *et al.* 1994; Wever *et al.* 1995; Wareham *et al.* 1997*a*).

Pankhurst (1982) noted that initial $^{87}Sr/^{86}Sr$ ratios of granitoids in Graham Land (Fig. 2) decrease systematically from *c.* 0.7065 in Mid-Jurassic times to *c.* 0.7040 in Tertiary times, and ascribed this trend to the waning influence of an unidentified pre-magmatic crustal component. Hole (1986) used the variation in initial $^{87}Sr/^{86}Sr$ ratios to define four groups of granitoids. Group I plutons (GL-I in Fig. 3a) range in composition from gabbro through diorite to granodiorite and granite. They were emplaced between 40 and 80 Ma, are restricted to the western archipelago of the Peninsula, and have low $^{87}Sr/^{86}Sr_i$ (0.7037–0.7045) and high εNd_i (0.8–5.5). Group II granodiorites (GL-II in Fig. 3a) are geographically widespread, were emplaced at *c.* 100 Ma, and have $^{87}Sr/^{86}Sr_i$ of *c.* 0.7048 and εNd_i of *c.* –0.8. Group III plutons (GL-III in

JOBNAME: JGS PAGE: 3 SESS: 33 OUTPUT: Wed Sep 26 15:06:45 2001
/hling/journals/geo/195/00139

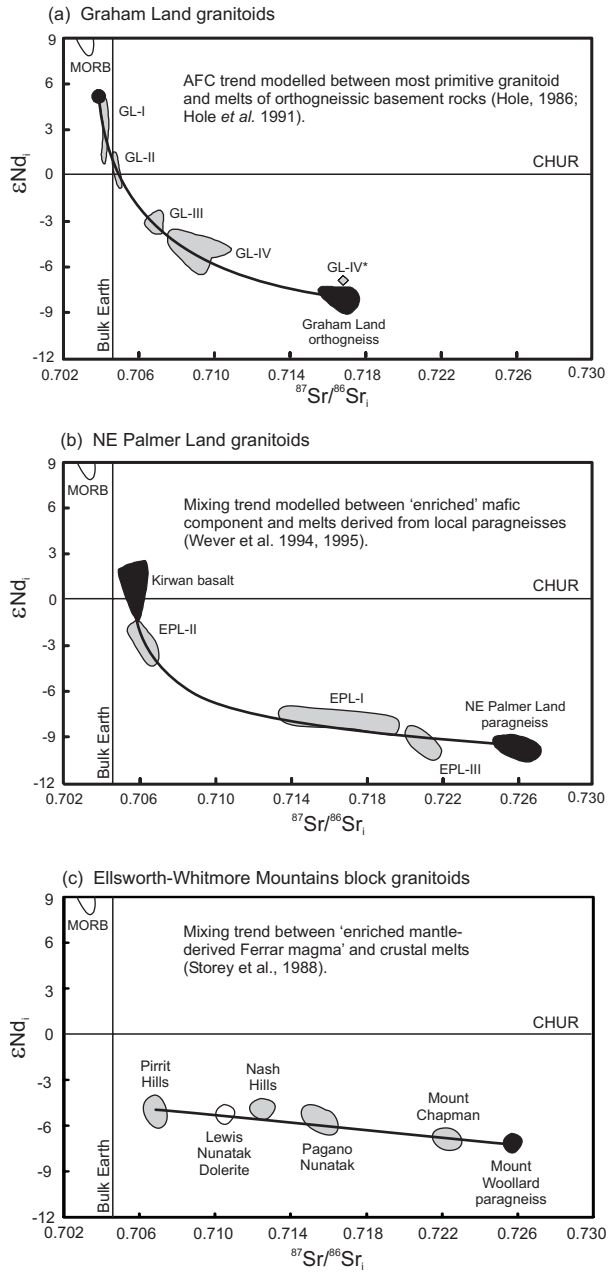

Fig. 3. Published models for variations in $^{87}Sr/^{86}Sr_i$ and εNd_i in granitoids of the Antarctic Peninsula and Ellsworth–Whitmore Mountains crustal blocks. See text for description of fields. In each case, melting of high-$^{87}Sr/^{86}Sr$ crust is invoked, although a variety of mafic end-members are suggested.

Fig. 3a) range in composition from diorite to granite. They were emplaced in central-eastern Graham Land between 160 and 209 Ma, and have $^{87}Sr/^{86}Sr_i$ between 0.7060 and 0.7068, and εNd_i between –2.3 and –3.7. Group IV plutons (GL-IV in Fig. 3a) are dominated by gabbro and granodiorite. They were emplaced in SE Graham Land between 160 and 204 Ma, and are characterized by high $^{87}Sr/^{86}Sr_i$ (0.7074–0.7094) and low εNd_i (–3.5 to –6.6). A single two-mica granite from Joerg Peninsula (Fig. 2) has unusually high $^{87}Sr/^{86}Sr_i$ (0.716 at 175 Ma), and was thought to be derived by partial melting of local gneissic basement rocks (GL-IV* in Fig. 3a; Hole 1986). Attempts were made to model the trend shown by the four groups of Graham Land granitoids in εSr_i–εNd_i space using assimilation-fractional crystallization modelling (AFC; DePaolo 1981; Hole 1986; Hole *et al.* 1991), and analyses of the most primitive observed granitoid and partial melts of gneissic basement as end-members (Fig. 3a). Acceptable fits could only be achieved using relatively high values for the rate of assimilation relative to fractional crystallization (r=0.9; Hole *et al.* 1991).

An alternative model for the formation of Graham Land granitoids was proposed by Storey & Alabaster (1991), who suggested that the majority of Early–Mid-Jurassic Group IV plutons may result from fractional crystallization of an enriched lithospheric mantle source, similar to that of the contemporaneous Ferrar and Karoo basalts.

Granitoids emplaced in NE Palmer Land (Fig. 2) during Triassic–Early Jurassic times show a wide range in isotope composition (Fig 3b; Wever *et al.* 1994, 1995). The earliest plutons form gneissic granites (EPL-I in Fig. 3b), whose protoliths were emplaced at *c.* 220 Ma. They have high $^{87}Sr/^{86}Sr_i$ (0.714 to 0.720) and low εNd_i (–7.4 to –8.1). A suite of metaluminous granites (EPL-II in Fig. 3b) was intruded at *c.* 210 Ma, and shows relatively low $^{87}Sr/^{86}Sr_i$ (*c.* 0.706) and high εNd_i (–1.9 to –3.4). Subsequently, highly peraluminous leucogranites (EPL-III in Fig. 3b) were emplaced at *c.* 205 Ma. These have very high $^{87}Sr/^{86}Sr_i$ (0.720–0.721) and low εNd_i (–8.8 to –9.4), and were derived, at least in part, by partial melting of local paragneiss (Fig. 3b). Wever *et al.* (1994) demonstrated that it is not possible to generate the observed range in granite composition by mixing of a MORB-like mantle end-member with melts of the paragneiss. However, Wever *et al.* (1995) showed that a solution could be achieved by mixing melts of paragneiss with an enriched (i.e. low εNd_i, high $^{87}Sr/^{86}Sr_i$) mafic end-member, similar in composition to the Kirwan basalt lavas of Dronning Maud Land, Antarctica, which chemically resemble the contemporaneous Karoo lavas of South Africa. (Fig. 3b). Granitoids of NW Palmer Land (Fig. 2) have also been considered to contain a significant component derived from pre-Triassic crust (Wareham *et al.* 1997*b*). In this area, the mafic end-member is thought to be derived by mixing of basaltic–andesitic arc magmas with melts of juvenile basaltic underplate at the base of the crust. The crustal end-member has been modelled using a locally exposed Triassic orthogneiss.

Leat *et al.* (1995) considered the Antarctic Peninsula batholith as a whole, and concluded that, whereas many S-like Jurassic granites contain a large component derived by melting of upper crust, granitoids emplaced during the Early Cretaceous intrusive peak were formed largely by melting of mafic–intermediate igneous lower crust. They suggested that the change in trace element and isotope composition between Jurassic and early Cretaceous plutons resulted from migration of the main zone of crustal melting, from dominantly upper crustal, sedimentary sources, to lower crustal, meta-igneous sources.

Mid-Jurassic granites of the adjacent Ellsworth–Whitmore Mountains crustal block (Fig. 1) are thought to be genetically related to the break-up of Gondwana (Storey *et al.* 1988). They have low εNd_i (–4.7 to –7.0) and variable $^{87}Sr/^{86}Sr_i$ (0.707–0.722), and range in composition from a within-plate granite end-member (Pirrit Hills granite; Fig. 3c) to granites with a more marked crustal signature (Mount Chapman granite; Fig. 3c). The high-$^{87}Sr/^{86}Sr_i$ granites plot close to the composition of local paragneissic basement rocks (Fig. 3c). Storey *et al.*

JOBNAME: JGS PAGE: 4 SESS: 33 OUTPUT: Wed Sep 26 15:06:45 2001
/hling/journals/geo/195/00139

Table 1. *Pb isotope data for leached feldspars from Antarctic Peninsula granitoids*

Sample	Rock type	Locality	Mineral	Age (Ma)	$^{206}Pb/^{204}Pb$	$^{207}Pb/^{204}Pb$	$^{208}Pb/^{204}Pb$
Graham Land							
BR.024.4	Diorite	Faure Islands	Pl	48	18.729	15.621	38.492
R.080.1	Granite	Horseshoe Island	Pl	67	18.796	15.634	38.566
R.312.2	Granite	Bildad Peak	Pl	163	18.569	15.658	38.441
R.326.2	Granodiorite	Mount Fritsche	Pl	164	18.640	15.649	38.510
R.2614.1	Two-mica granite	Curran Bluff	Pl	204	18.735	15.664	38.695
R.349.1	Granodiorite gneiss	Adie Inlet	Pl	?550	18.566	15.668	38.460
R.3632.2	Metagranite	Marsh Spur	Pl	325	18.468	15.616	38.164
R.5511.1	Gneiss	Target Hill	Pl	392	18.985	15.660	38.535
NW Palmer Land							
R.5256.1	Granite	Mount Pitman	Pl	60	18.751	15.616	38.504
R.5736.1	Granodiorite	Scorpio Peaks	Kfs	70	18.725	15.609	38.452
R.5796.4	Granodiorite	Cetus Hill	Pl	120	18.757	15.636	38.522
R.3216.3	Tonalite	Burns Bluff	Pl	140	18.701	15.658	38.546
R.5284.1	Granodiorite	Renner Peak	Pl	140	18.683	15.633	38.483
R.6057.10	Gabbro	Burns Bluff	Pl	141	18.571	15.623	38.370
R.5287.1	Diorite	Creswick Peaks	Pl	141	18.681	15.637	38.508
R.5270.1	Diorite	Goettel Escarpment	Pl	182	18.644	15.646	38.463
R.5271.4	Foliated granite	Goettel Escarpment	Kfs	183	18.641	15.647	38.476
R.5504.2	Foliated granodiorite	Auriga Nunataks	Kfs	203	18.741	15.650	38.543
R.5278.8	Granite gneiss	Campbell Ridges	Kfs	227	18.707	15.654	38.604
NE Palmer Land							
R.4908.10	Leucogranite gneiss	Mount van Buren	Pl	206	18.679	15.655	38.446
R.5006.7	Metagranodiorite	Pinther Ridge	Pl	209	18.669	15.657	38.532
R.4942.4	Metagranodiorite	Hall Ridge	Pl	211	18.802	15.662	38.626
R.4552.9	Leucogranite gneiss	Mount Nordhill	Pl	220	18.715	15.661	38.512
R.4920.12	Megacrystic granite	Mount Nordhill	Pl	220	18.694	15.672	38.545

Pl, plagioclase; Kfs, K-feldspar.

(1988) concluded that the within-plate granite end member could be derived entirely by differentiation of an enriched, mantle-derived Ferrar-like magma.

Analytical methods

Powders for geochemical analysis were prepared from 2–3 kg of fresh rock. Samples were reduced to *c.* 3 cm^3 chips using a hardened-steel hydraulic splitter, then crushed in a hardened-steel jaw-crusher. Powders were produced using an agate Tema-mill. Sr, Nd and Pb isotope analyses were carried out at the NERC Isotope Geosciences Laboratory, Keyworth. Rb–Sr and Sm–Nd analysis followed procedures described by Pankhurst *et al.* (1993); Pankhurst & Rapela (1995). $^{87}Sr/^{86}Sr$ ratios are normalized to $^{86}Sr/^{88}Sr=0.1194$, and $^{143}Nd/^{144}Nd$ ratios are normalized to $^{146}Nd/^{144}Nd=0.7219$. Long-term reproducibility of Sr and Nd isotope ratios in standard solutions is 15–20 ppm (1σ), but on rock standards this rises to 30–40 ppm. Sr results are normalized to a value of 0.710240 for NBS987, to allow comparison with earlier datasets. Pb isotope ratios were determined on 10–50 mg of handpicked plagioclase and potassium feldspar. Feldspars have extremely low U/Pb and Th/Pb, so that changes in their Pb isotope ratios, due to *in situ* decay of U and Th, are small. Nonetheless, an easily leachable, relatively radiogenic Pb component is often present, suggesting that feldspar rarely remains closed to the addition and loss of U, Th and Pb (e.g. Gariépy & Allègre 1985; Sultan & Bickford 1992). In order to remove this component, the feldspars were leached in hot 6N HCL for one hour, then washed in deionized water and powdered with an agate mortar and pestle (cf. Gariépy & Allègre 1985). The feldspar powders were then leached in an ultrasonic bath for five minutes in 5% HBr + 5% HF, and washed several times with deionized water prior to dissolution.

Pb analyses followed procedures summarized in Kempton & Downes (1997) Kempton *et al.* (1997). Pb isotope ratios are corrected for fractionation using the standard values of Todt *et al.* (1984). Long-term reproducibility of Pb isotope ratios in the NBS981 solution standard is better than $\pm 0.2\%$ (2σ). Long term reproducibility of the BHVO-1 rock standard is better than $\pm 0.4\%$ (2σ). Laboratory blanks for Sr, Nd and Pb at the time of analysis were better than 500, 250, and 170 pg, respectively.

Oxygen isotope ratios were determined by conventional fluorination after the procedure of Clayton & Mayeda (1963). Sample decomposition was carried out with chlorine trifluoride, and the resultant oxygen reacted with hot graphite to produce carbon dioxide, the isotopic composition of which was determined using a VG SIRA 10 mass spectrometer. The accuracy of the technique was confirmed by periodic analysis of standard NBS 28 (African Glass Sand +9.6‰), with reproducibility being better than ± 0.3‰.

Sample selection

This study combines new Sr, Nd, Pb, and O isotope data with a review of published data. Samples were selected from granitoids emplaced throughout the history of subduction-related magmatism along the Antarctic Peninsula, and spanning the time of Gondwana break-up. All published data were re-evaluated in order to maximize the reliability of the trends displayed. The ages of certain key samples have been verified using U–Pb zircon analysis, in order to minimize scatter caused by inaccurate age correction. Samples whose ages could not be reliably estimated have been excluded from the data set. Samples with high $^{87}Rb/^{86}Sr$ (>25) have also been excluded, unless their ages are known precisely. The error in calculated $^{87}Sr/^{86}Sr_i$ for these samples is > 0.001 for each three million years of uncertainty in the age, contributing significantly to scatter in the observed trends.

For Pb-isotope analysis, plutons showing the widest possible range in Sr and Nd isotope compositions were selected. A number of pre-Mesozoic lithologies were also analysed, in order to constrain possible crustal end-members. These included Silurian orthogneiss from Eastern Graham Land, and pre-Triassic paragneiss from Eastern Palmer Land.

In order to allow comparison of granitoids from the Antarctic Peninsula and adjacent areas, data have been grouped by geological Period. The Phanerozoic time-scale of Gradstein & Ogg (1996) is used

JOBNAME: JGS PAGE: 5 SESS: 33 OUTPUT: Wed Sep 26 15:06:45 2001
/hling/journals/geo/195/00139

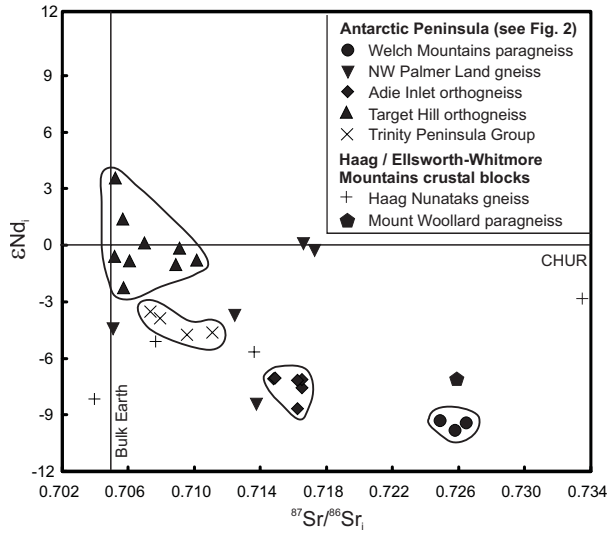

Fig. 4. $^{87}Sr/^{86}Sr_i$ and εNd_i characteristics of basement rocks of the Antarctic Peninsula and adjacent crustal blocks recalculated at 200 Ma.

throughout. Pb isotope data are presented in Table 1. The full Sr and Nd data set, incorporating 45 previously unpublished analyses, 55 analyses from unpublished PhD theses, and 58 published analyses, can be obtained from the Society Library or the British Library Document Supply Centre, Boston Spa, Wetherby, West Yorkshire LS23 7BQ, UK as Supplementary Publication No. SUP 18161 (6 pages).

Sr and Nd isotope data

Pre-Triassic basement

The Sr and Nd isotope characteristics of Antarctic Peninsula basement rocks are shown in Figure 4, recalculated at 200 Ma. Paragneisses from the Welch Mountains in NE Palmer Land (Fig. 2) show the strongest upper crustal signature, with high $^{87}Sr/^{86}Sr_i$ and low εNd_i. These paragneisses contain abundant detrital zircons ranging in age from *c.* 500 to *c.* 1800 Ma (Millar, Pankhurst & Fanning, unpublished data) and have depleted mantle Nd model ages of *c.* 1700 Ma, suggesting derivation from a source within Gondwana.

Orthogneisses from Adie Inlet in E Graham Land also have high $^{87}Sr/^{86}Sr_i$ and low εNd_i, (Fig. 4), and are thought to represent Mid-Cambrian granites which underwent metamorphism during Early Triassic times (Millar *et al.* in press). They contain abundant Proterozoic inherited zircon, and have Middle Proterozoic Nd model ages (*c.* 1600 Ma).

Gneissic basement rocks from NW Palmer Land represent a variety of Palaeozoic granitoids that underwent intense metamorphism and migmatization during Mid–Late Triassic times. The U–Pb zircon systematics of these rocks are dominated by high-U overgrowths which record the time of migmatization. Protolith ages ranging from Cambrian to Devonian are recorded by SHRIMP analyses of grain cores (Millar *et al.* in press). The NW Palmer Land gneisses scatter widely on a plot of εNd_i against $^{87}Sr/^{86}Sr_i$ (Fig. 4), reflecting heterogeneity induced by Triassic migmatization.

Orthogneissic basement rocks from Target Hill, E Graham Land (Fig. 2) were emplaced in Silurian–Devonian times (Milne & Millar 1989). They have relatively low $^{87}Sr/^{86}Sr_i$ and high εNd_i at 200 Ma (Fig. 4), and show low depleted mantle Nd model ages (*c.* 1000 Ma). The relatively primitive nature of these rocks is confirmed by the absence of inherited zircon (Millar *et al.* in press).

NW Palmer Land granitoids

In NW Palmer Land, granitoids emplaced between *c.* 230 Ma and 60 Ma show a wide range in $^{87}Sr/^{86}Sr_i$ (from 0.7042 to 0.7089) and εNd_i (from +4.5 to –6.5), and fall on a steep curve on a plot of εNd_i against $^{87}Sr/^{86}Sr_i$ (Fig. 5a).

Upper Cretaceous–Cenozoic granitoids in NW Palmer Land area occur as hypabyssal granite sheets within thick volcanic successions. They have relatively low $^{87}Sr/^{86}Sr_i$ (0.7043 to 0.7066) and high εNd_i (+4.4 to –2.1). Granitoids that were emplaced in earliest Cretaceous times at around 140 Ma show a wide range in Sr and Nd isotope characteristics. Arc magmatism was particularly voluminous at *c.* 140 Ma, with extensive emplacement of granitoids ranging from hornblende gabbro to leucogranite within crustal-scale extensional shear zones (Vaughan & Millar 1996; Vaughan *et al.* 1997). Isotope compositions show a wide range, with $^{87}Sr/^{86}Sr_i$ between 0.7042 and 0.7069 and εNd_i between +4.2 and –3.0 (Fig. 5a; Wareham *et al.* 1997*a, b*). Granitoids emplaced between Late Triassic and Mid-Jurassic times have relatively high $^{87}Sr/^{86}Sr_i$ (0.7058–0.7089) and low εNd_i (–0.3 to –6.5); Middle Jurassic granites from the Batterbee Mountains (Fig. 2) show the highest $^{87}Sr/^{86}Sr_i$ and lowest εNd_i.

Graham Land granitoids

The Sr and Nd isotope characteristics of Graham Land granitoids have previously been described in terms of two-component AFC mixing between a mantle-derived end-member, and melts of orthogneissic basement (Hole 1986; Hole *et al.* 1991; Fig. 3a). Here, the data of Hole (1986) are re-evaluated together with nine new analyses from Marguerite Bay, SW Graham Land. With few exceptions, the Graham Land granitoids plot on the same steep trend shown by the NW Palmer Land data (Fig. 5a,b).

Granitoids emplaced during Cretaceous and Cenozoic times are restricted to the western coast of Graham Land. They have relatively low $^{87}Sr/^{86}Sr_i$ (0.7037 to 0.7063) and high εNd_i (5.3 to –2.5), and fall on a steep trend on plot of εNd_i against $^{87}Sr/^{86}Sr_i$ (Fig. 5b). There is a systematic decrease in $^{87}Sr/^{86}Sr_i$ and increase in εNd_i with decreasing age of emplacement. Plutons emplaced in eastern Graham Land during Early to Mid-Jurassic times have relatively high $^{87}Sr/^{86}Sr_i$ (0.7061–0.7138) as well as low εNd_i (–2.2 to –6.2) (Fig. 5b). The majority of the data plot on an extension of the steep trend shown by the data from Cretaceous and Tertiary granitoids. The low-εNd_i end of the dominant steep trend is marked by gabbros from Joerg Peninsula (Fig. 2), which have $^{87}Sr/^{86}Sr_i$ values between 0.7080 and 0.7090, and εNd_i between –4.1 and –6.1. A few analyses of Early–Mid-Jurassic granitoids from Joerg Peninsula plot to the right of this trend, on a vector towards the field defined by pre-Mesozoic metamorphic basement rocks. Two samples from a granite intruding gneisses at Curran Bluff, Joerg Peninsula (Fig. 2), plot well to the right of the dominant trend, with $^{87}Sr/^{86}Sr_i$ as high as 0.7138 and εNd_i=–6.2 (calculated at a preferred age of 204 Ma; cf. Hole 1986). This granite has previously been interpreted as a partial melt of the Neoproterozoic Adie Inlet gneiss, which crops out some 150 km to the north, in eastern Graham Land

JOBNAME: JGS PAGE: 6 SESS: 33 OUTPUT: Wed Sep 26 15:06:45 2001
/hling/journals/geo/195/00139

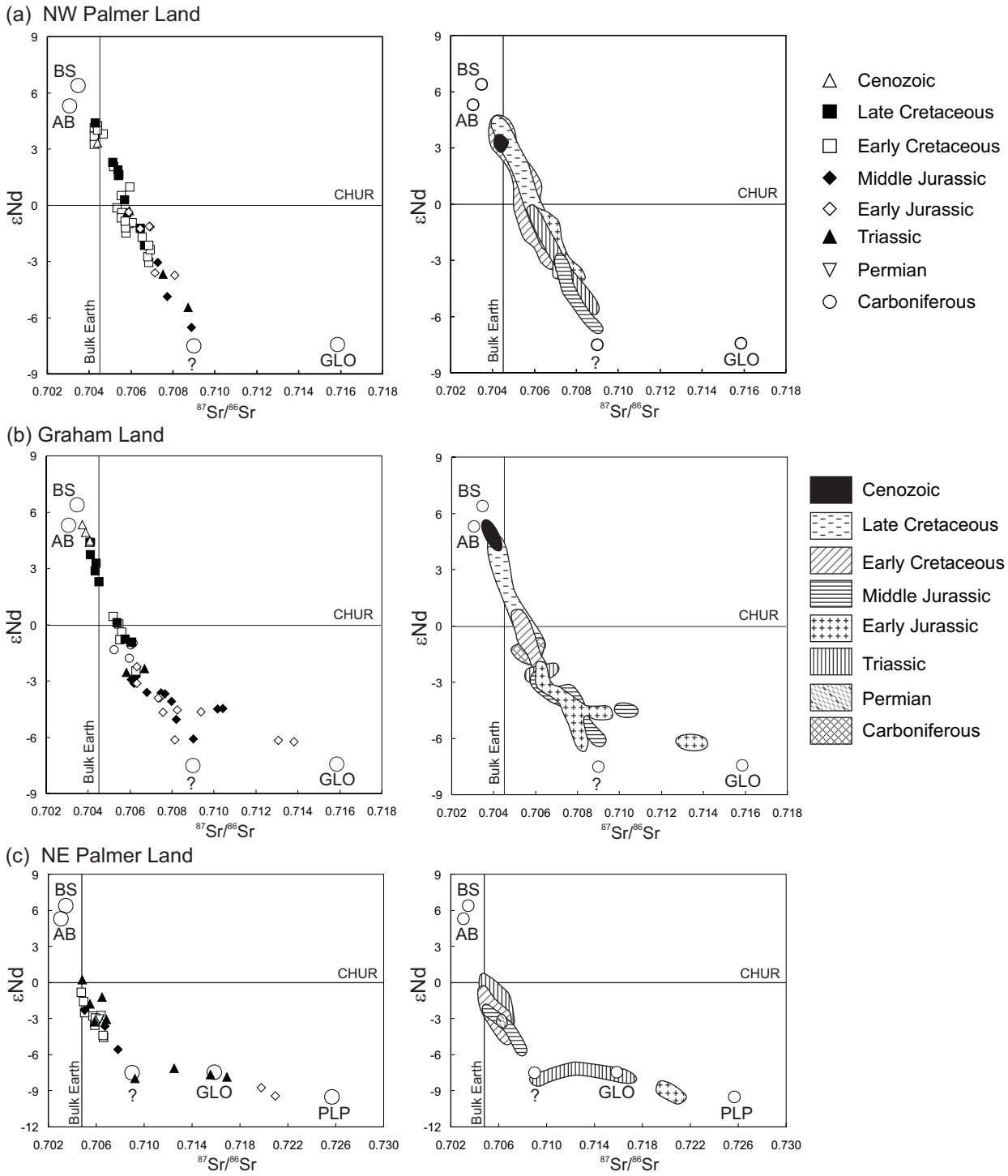

Fig. 5. Plots of εNd_i against $^{86}S_i/^{87}S_{ri}$ for granitoids of (**a**) NW Palmer Land, (**b**) Graham land and (**c**) NE Palmer Land. BS, Bransfield Strait basalts; AB, post-subduction alkali basalts; TH, Target Hill Silurian–Devonian granitoids; GLO, Graham Land orthogneiss (Adie Inlet gneiss) calculated at 200 Ma. PLP, Palmer Land paragneiss (Welch Mountains), calculated at 200 Ma. The field marked '?' represents a proposed lower crustal end-member.

(Pankhurst *et al.* 1983; Hole 1986). The Curran Bluff granite forms a small boss within Triassic gneisses and undated metasedimentary rocks. It seems more likely that the granite is formed by melting of these lithologies, which, themselves, have a considerable pre-Mesozoic history as reflected by their complex inherited zircon population (Millar, Pankhurst & Fanning, unpublished data).

Two analyses of Late Triassic granite have been obtained from Graham Land, from widely separated outcrops at Cole Peninsula, in eastern Graham Land, and Elton Hill in south-westernmost Graham Land (Fig. 2). These granites have similar isotope characteristics ($^{87}Sr/^{86}Sr_i$=*c.* 0.7063, $\varepsilon Nd_i \approx$ –2.4), and plot on the steep trend shown by the bulk of the Graham Land data (Fig. 5b). Carboniferous granites from

JOBNAME: JGS PAGE: 7 SESS: 33 OUTPUT: Wed Sep 26 15:06:45 2001
/hling/journals/geo/195/00139

Table 2. *O-isotope composition of granitoids from the Ellsworth–Whitmore Mountains crustal block*

Sample	Rock type	Locality	$\delta^{18}O_{SMOW}$		
			Whole-rock	Quartz	Plagioclase
R.2243.4	Granite	Pirrit Hills	9.1	10.0	9.0
R.2226.4	Granite	Linck Nunatak	10.0		
R.2215.4	Granite	Pagano Nunatak	10.1	11.7	9.9

eastern Graham Land also plot on the dominant trend, with $^{87}Sr/^{86}Sr_i \approx 0.7060$ and $\varepsilon Nd_i \approx -1.3$ (Fig. 5b).

In summary, the majority of the analysed Carboniferous to Tertiary granitoids from Graham Land plot on a steep trend in $^{87}Sr/^{86}Sr_i$–εNd_i space. The trend shown by the Graham Land granitoids is identical to that shown by the NW Palmer Land rocks (Fig. 5a,b). Only five analyses, representing three granite bodies outcropping within an area of 15×15 km on Joerg Peninsula (Fig. 2), fall to the right of the dominant steep trend. These granite bodies are spatially associated with gabbros, which themselves plot on the dominant steep trend.

NE Palmer Land granitoids

In NE Palmer Land, granitoids showing a wide range in Sr and Nd isotope compositions were emplaced between Late Triassic and Early Cretaceous times (Wever *et al.* 1994; Scarrow *et al.* 1996). Late Triassic foliated granites and Mid-Jurassic diorites and granites from the area between Mount Charity (Fig. 2) and the Welch Mountains have relatively low $^{87}Sr/^{86}Sr_i$ (0.7050–0.7078) and high εNd_i (0.2 to –3.5), and plot on a steep trend similar to that defined by Graham Land and NW Palmer Land granitoids. In contrast, Late Triassic biotite orthogneiss and megacrystic granite from the Welch Mountains, and Early Jurassic foliated leucogranite from Mount Jackson (Fig. 2), plot on a prominent near-horizontal trend towards high $^{87}Sr/^{86}Sr_i$ values typical of local paragneiss (Fig. 5c). Middle Jurassic and Early Cretaceous granites from NE Palmer Land define distinct, steeply oriented fields in $^{87}Sr/^{86}Sr_i$–εNd_i space, straddling the dominant, steep trend shown by Graham Land and NW Palmer Land granitoids (Fig. 5c).

Summary of Sr and Nd data

The majority of Palaeozoic–Tertiary plutons from Graham Land and NW Palmer Land plot on steep, non-curvilinear trends on plots of εNd_i against $^{87}Sr/^{86}Sr_i$. Only a few, geographically restricted plutons plot on trends towards high-$^{87}Sr/^{86}Sr_i$ compositions typical of local basement rocks. Plutons from NE Palmer Land also appear to plot on two distinct trends on plots of εNd_i against $^{87}Sr/^{86}Sr_i$, rather than on a single, concave upwards mixing curve. It is not possible to generate mixing or AFC curves that encompass the full range of the granitoid data. Rather, it is suggested that the majority of the granitoids are derived by mixing of a high-εNd_i, low-$^{87}Sr/^{86}Sr_i$ mafic component, derived from the mantle or basaltic underplate, with a low-εNd_i, moderate-$^{87}Sr/^{86}Sr_i$ component, resulting in the steep trends seen in Figure 5. Melting of a high-$^{87}Sr/^{86}Sr_i$, low εNd_i component was only of localized importance during Triassic–Mid-Jurassic times, giving rise to the extended, flat-lying trends in Figure 5.

Pb isotope data

Antarctic Peninsula granitoids show a restricted range of Pb isotope compositions (Table 2). $^{206}Pb/^{204}Pb_i$ ranges from 18.47 to 18.98, while $^{207}Pb/^{204}Pb_i$ and $^{208}Pb/^{204}Pb_i$ range from 15.61 to 15.67 and 38.16 to 38.63, respectively. The data plot above the Northern Hemisphere Reference Line (Fig. 6), and straddle the various Pb growth curves for crustal rocks. The pluton compositions overlap with the fields for Antarctic Peninsula sulphide (Willan & Swainbank, 1995), and the Bransfield Strait marginal basin basalts (Fig. 6; Keller *et al.* 1991). Post-subduction alkali basalts from the Antarctic Peninsula have considerably higher $^{206}Pb/^{204}Pb_i$ and $^{208}Pb/^{204}P_i$ than the granitoids (Fig. 6).

There is a systematic decrease in pluton $^{207}Pb/^{204}Pb_i$ composition between Triassic and Cenozoic times (Fig. 7b). Pluton $^{206}Pb/^{204}Pb_i$ and $^{208}Pb/^{204}Pb_i$ compositions do not show steady growth through time. Instead, $^{206}Pb/^{204}Pb_i$ and $^{208}Pb/^{204}Pb_i$ decrease between Triassic and earliest Cretaceous times. $^{206}Pb/^{204}Pb_i$ then increases during Early Cretaceous and Cenozoic times, while $^{208}Pb/^{204}Pb_i$ shows no systematic variation (Fig. 7 a,c). Cenozoic Pb-isotope compositions are similar to the values shown by Bransfield Strait marginal basin basalts (BS in Fig. 7). Triassic granitoids have similar $^{207}Pb/^{204}Pb_i$ to typical Graham Land orthogneiss (GLO in Fig. 7), but slightly more radiogenic $^{206}Pb/^{204}Pb_i$.

Plots of $^{206}Pb/^{204}Pb_i$ and $^{208}Pb/^{204}Pb_i$ against $^{87}Sr/^{86}Sr_i$ show no systematic correlation. However, $^{207}Pb/^{204}Pb_i$ varies systematically with $^{87}Sr/^{86}Sr_i$ (Fig. 8). The majority of Early Jurassic–Tertiary plutons plot on a steep trend of increasing $^{207}Pb/^{204}Pb_i$ with increasing $^{87}Sr/^{86}Sr_i$ (Trend 1). A few Triassic–Early Jurassic plutons fall on a trend of decreasing $^{207}Pb/^{204}Pb_i$ with increasing $^{87}Sr/^{86}Sr_i$ (Trend 2) towards values expected of exposed gneissic basement rocks. It is not possible to model the entire dataset as resulting from mixing of a Bransfield-Strait-like mantle source with high $^{207}Pb/^{204}Pb_i$, high $^{87}Sr/^{86}Sr_i$ upper crust. Rather, Trend 1 is thought to reflect mixing of a Bransfield-Strait-like basaltic end-member with a relatively high $^{207}Pb/^{204}Pb_i$, moderate $^{87}Sr/^{86}Sr_i$ end-member. Melting and assimilation of a high $^{87}Sr/^{86}Sr_i$ component was only involved in the formation of a few Triassic–Early Jurassic plutons, which plot on Trend 2.

O isotope data

Mixing relationships on plots of $\delta^{18}O$ against $^{87}Sr/^{86}Sr_i$ provide a useful method for distinguishing between melts which have assimilated continental crust, and melts derived from a contaminated mantle source containing, for example, a subducted sediment component (James 1981). The Sr-isotope signatures of partial melts of subduction-modified mantle should, in principle, be dominated by the easily fusible, relatively high-Sr

JOBNAME: JGS PAGE: 8 SESS: 33 OUTPUT: Wed Sep 26 15:06:45 2001
/hling/journals/geo/195/00139

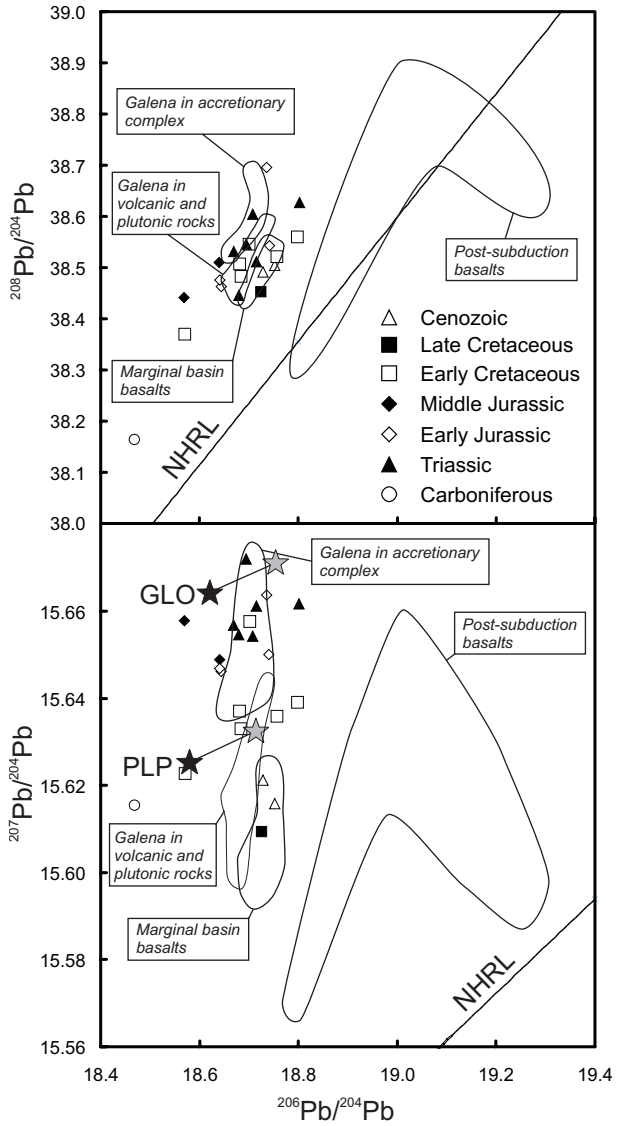

Fig. 6. (**a**) Plot of $^{207}Pb/^{204}Pb_i$ v. $^{206}Pb/^{204}Pb_i$ and (**b**) plot of $^{208}Pb/^{204}Pb_i$ v. $^{206}Pb/^{204}Pb_i$ for granitoids of the Antarctic Peninsula. NHRL, Northern Hemisphere Reference Line. Growth curves for Graham Land orthogneiss (GLO) and Palmer Land paragneiss (PLP) are shown between 230 and 100 Ma. The data show a restricted range in Pb-isotope composition. However, the granitoids fall on a broad trend between a mafic end member, represented by the Bransfield Straits marginal basin basalts, and compositions typical of gneissic basement.

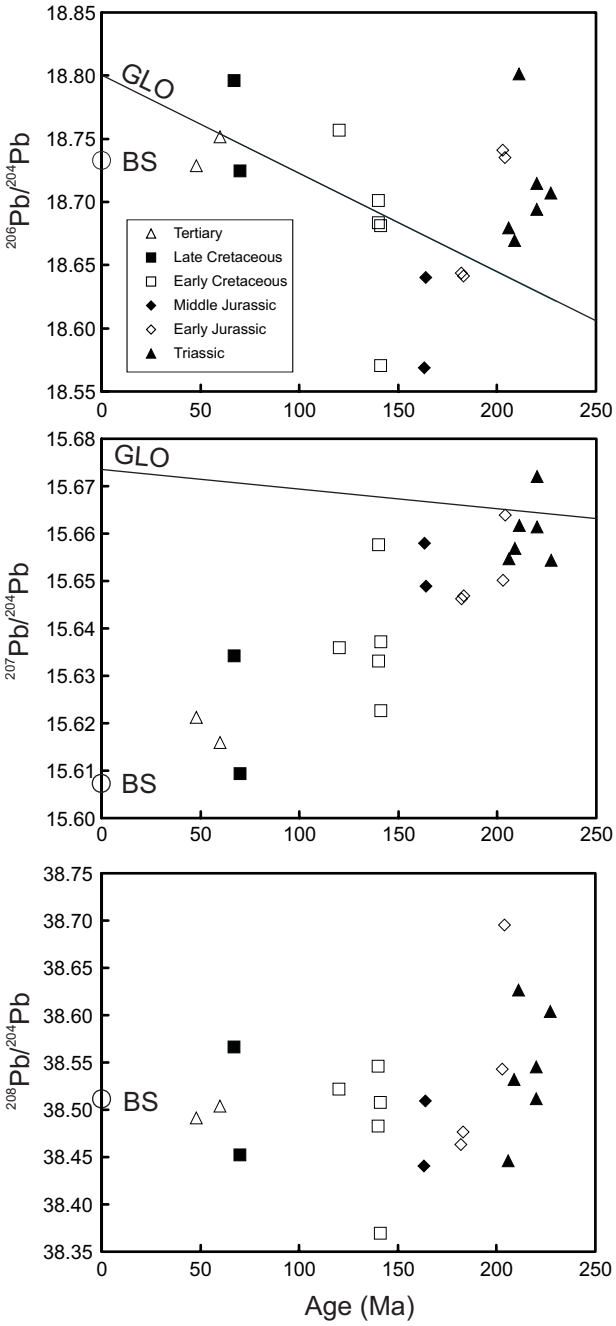

Fig. 7. Variation in Pb isotope composition of Antarctic Peninsula granitoids through time. BS, Bransfield Strait marginal basin basalts; GLO, growth curve for Graham Land orthogneiss.

component derived from the slab, resulting in convex-downwards curves on $\delta^{18}O$–$^{87}Sr/^{86}Sr_i$ plots (Fig. 9). In contrast, assimilation of melts derived from continental crust, with Sr concentrations the same or lower than those in the magma will result in convex upwards mixing curves. Molzahn *et al.* (1996) used this relationship to suggest that the Ferrar flood basalts of Victoria Land were derived from a lithospheric mantle source which was enriched in material derived from the continental crust, perhaps in the form of subducted sediments (Fig. 9). Published data for the Ferrar and Kirwan basalts satisfy a similar relationship (Kyle *et al.* 1983; Harris *et al.* 1990; see Fig. 9). In contrast, whole-rock oxygen data for Antarctic Peninsula granitoids (Hole 1986) fall on convex upward $\delta^{18}O$–$^{87}Sr/^{86}Sr_i$ mixing curves, confirming that their composition is controlled by crustal contamination processes (Fig. 9). Samples from a Late Cretaceous granite from Horseshoe Island, Marguerite Bay (Fig. 2) have very low $\delta^{18}O$ values, suggesting that they have interacted with meteoric water. The majority of the remaining data fall on a steep trend, which can be modelled as resulting from simple mixing of a mantle derived component, and a moderate $^{87}Sr/^{86}Sr_i$, high $\delta^{18}O$ component (Fig. 9). A single analysis of a high $^{87}Sr/^{86}Sr_i$ Mid-Jurassic granite from eastern Graham Land plots on a vector between a moderate $^{87}Sr/^{86}Sr_i$, high $\delta^{18}O$ component

JOBNAME: JGS PAGE: 9 SESS: 33 OUTPUT: Wed Sep 26 15:06:45 2001
/hling/journals/geo/195/00139

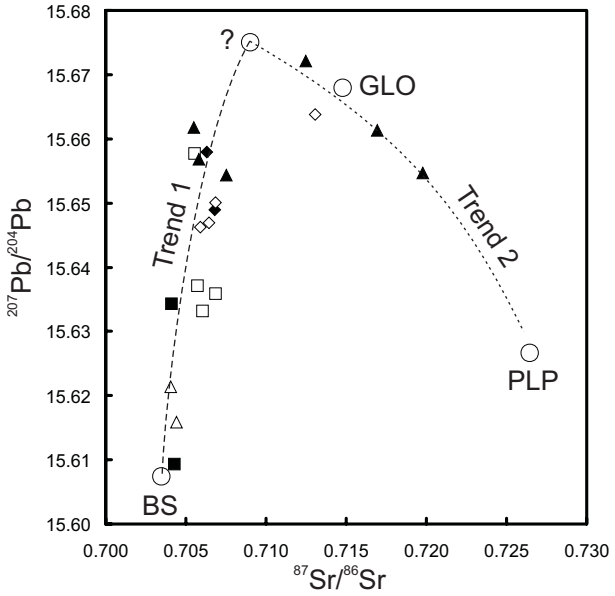

Fig. 8. Plot of $^{207}Pb/^{204}Pb_i$ against $^{87}Sr/^{86}Sr_i$. The majority of Early Jurassic–Tertiary plutons plot on a steep trend (Trend 1) between a Bransfield Strait-like basaltic end-member (BS) and a high $^{207}Pb/^{204}Pb_i$, moderate $^{87}Sr/^{86}Sr_i$ end-member (?). A few Triassic–Early Jurassic plutons fall on a trend of decreasing $^{207}Pb/^{204}Pb_i$ with increasing $^{87}Sr/^{86}Sr_i$ (Trend 2) towards values expected of exposed gneissic basement rocks (GLO, Graham Land orthogneiss; PLP, Palmer Land paragneiss).

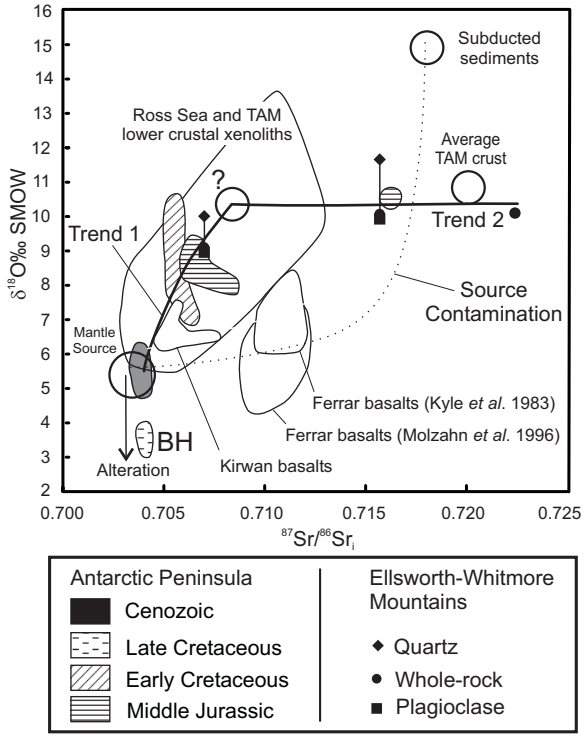

Fig. 9. Plot of $\delta^{18}O$ against $^{87}Sr/^{86}Sr_i$, showing mixing curves for source contamination and crustal contamination. TAM, Transantarctic Mountains; BH, Beacon Head granite, Horseshoe Island. Whereas the Ferrar and Kirwan basalts plot on concave-upwards curves, indicative of source contamination (dotted line), granitoids of the Antarctic Peninsula lie on a steep, concave downwards trend (Trend 1), suggesting assimilation of melts derived from continental crust. Granitoids from the Ellsworth–Whitmore Mountains crustal block, together with a single sample from the Antarctic Peninsula, lie on a shallow trend with constant, high $\delta^{18}O$ (Trend 2), suggesting derivation from sources entirely within the crust.

and values typical of average Transantarctic Mountains crust (Fig. 9). It is theoretically possible to fit a single mixing/AFC curve through all of the Antarctic Peninsula granitoid data on Figure 9. However, taking into account the Sr, Nd and Pb data presented above, the most straightforward explanation is that the majority of the Antarctic Peninsula granitoids fall on a mixing curve between mantle values and a low $^{87}Sr/^{86}Sr_i$, relatively high $^{207}Pb/^{204}Pb_i$, high $\delta^{18}O$ end-member. As was shown by the Sr–Nd isotope data, only a very few samples show evidence for assimilation of a high $^{87}Sr/^{86}Sr_i$ end member.

Also shown on Figure 9 are mineral and whole-rock analyses from granites of the Ellsworth–Whitmore Mountains crustal block (Fig. 1; Table 2), which lies adjacent to the Antarctic Peninsula. These granites have low εNd_i (*c.* –5.5) and variable $^{87}Sr/^{86}Sr_i$ (0.707–0.722), and have been interpreted as within-plate granites associated with the break-up of Gondwana (Storey *et al.* 1988). The Ellsworth–Whitmore Mountains granites clearly involve anatectic melts of crustal material (Fig. 3c). Storey *et al.* (1988) suggested that the mafic end-member in the formation of the Ellsworth–Whitmore Mountains granite suite may have been Ferrar-type basaltic magma, derived from an enriched lithospheric mantle source. Mixing relationships between $\delta^{18}O$ and $^{87}Sr/^{86}Sr_i$ suggest that this is not the case (Fig. 9). Whereas Ferrar basalts plot on convex downwards mixing curves, typical of source contamination, the Ellsworth–Whitmore Mountains granites plot on a trend between a high $\delta^{18}O$, moderate $^{87}Sr/^{86}Sr_i$ end member similar to that inferred from the Antarctic Peninsula granitoid data, and values typical of upper crust. The high $\delta^{18}O$ value of both end-members, and the shape of the mixing curve, suggest that the Ellsworth–Whitmore Mountains granites were formed by melting processes entirely within the crust, although the heat source was presumably supplied by crustal attenuation and mafic magmatism associated with the break-up of Gondwana. A similar origin is suggested for the low εNd, high-$^{87}Sr/^{86}Sr_i$ granites of the Antarctic Peninsula.

Crustal and mantle reservoirs

The isotope characteristics of Antarctic Peninsula granitoids suggest that they are derived by melting of subduction-modified lithospheric mantle, or basaltic underplate derived therefrom, and two distinct low-εNd_i high $\delta^{18}O$ crustal reservoirs that can be distinguished on the basis of their initial $^{87}Sr/^{86}Sr$ characteristics.

Subduction-modified mantle

A reasonable analogue for the expected composition of basalts derived from subduction-modified lithospheric mantle beneath the Antarctic Peninsula is supplied by the Quaternary marginal basin basalts of Bransfield Strait (Fig. 2). The Bransfield Strait basalts have $^{87}Sr/^{86}Sr$ between 0.7030 and 0.7035, εNd between 4.7 and 7.4, and show a restricted range in Pb-isotope compositions. $^{206}Pb/^{204}Pb$ ranges from 18.74 to 18.76, $^{207}Pb/^{204}Pb$

JOBNAME: JGS PAGE: 10 SESS: 33 OUTPUT: Wed Sep 26 15:06:45 2001
/hling/journals/geo/195/00139

from 15.60 to 15.62, and $^{208}Pb/^{204}Pb_i$ from 38.50 to 38.56 (Keller *et al.* 1991). No O-isotope data are available for the Bransfield Strait basalts. The chemical and isotope characteristics of the basalts can be explained by contamination of a depleted mantle source with a few percent of material derived from continental crust, recycled into the mantle via the subduction zone (Keller *et al.* 1991). The high Pb concentration in subducted sediment (13–52 ppm) relative to depleted mantle (0.043 ppm) means that the Pb-isotope signature of the basalts is dominated by the subducted sediments. Pb isotopes show considerably less range than the Sr and Nd isotope data, implying that both the mantle and sedimentary components have homogeneous Pb isotope ratios (Keller *et al.* 1991). The Bransfield Straits basalts plot on extensions of the trends shown by the Antarctic Peninsula granitoids on plots involving Sr, Nd and Pb isotopes (Figs 5, 6, 7 & 8).

The trend shown by Antarctic Peninsula granitoids, together with granites from the Ellsworth–Whitmore Mountains crustal block, on a plot of $\delta^{18}O$ against $^{87}Sr/^{86}Sr_i$, suggests that Ferrar-type 'enriched' mantle is not a suitable mantle source for the granitoid magmas in either area (cf. Storey *et al.* 1988; Wever *et al.* 1995).

Crustal components

The continental crust of the Antarctic Peninsula is the product of a long and complex tectonomagmatic history. Recent studies have suggested that the peninsula is composed of a number of terranes (Vaughan & Storey 2000), including an eastern terrane which formed part of the Pacific margin of Gondwana, and a number of marginal terranes, which may represent accreted microcontinental rocks and oceanic sediments. It is clear that the few examples of pre-Mesozoic basement rocks exposed within the magmatic arc give only a hint of the complexity of the pre-Mesozoic basement of the peninsula.

In order to assess possible crustal end-members in the genesis of Antarctic Peninsula granitoids, it is necessary to consider the broad variation in composition within the crust: in particular, the geochemical and isotopic differences between upper and lower crustal compositions (e.g. Taylor & McLennan 1995).

The present composition of the upper crust is largely the result of intracrustal differentiation, leading to the production of granites *s.l.* (Taylor & McLennan, 1995). The upper crust has a broadly granodioritic composition, and contains high abundances of large-ion lithophile elements (including Rb), leading to high time-integrated $^{87}Sr/^{86}Sr$. In general, granites formed by melting of sedimentary rocks will have high $\delta^{18}O$.

In contrast, the composition of the lower crust may be controlled by a complex sequence of processes driven by basaltic underplating, leading to 'blending of sub-crustal and deep crustal magmas in zones of melting, assimilation, storage and homogenization' (MASH: Hildreth & Moorbath 1988). Many lower crustal granulite xenoliths appear to represent the products of large-scale hybridization of differentiating mantle-derived melts and mafic restites after metasediment anatexis and granite genesis (Kempton & Harmon 1992). The lower crust is characterized by low Rb/Sr (Taylor & McLennan, 1995), leading to low time-integrated $^{87}Sr/^{86}Sr$. $\delta^{18}O$ values in lower crustal xenoliths are highly variable (+5.4 to +13.5 ‰), the highest values being shown by silicic metaigneous granulites and metasedimentary granulites (Kempton & Harmon 1992).

The isotope data presented here for Antarctic Peninsula granitoids suggest that two distinct crustal sources are involved in their genesis. The dominant crustal component (Crust 1) has low εNd_i; moderate $^{87}Sr/^{86}Sr_i$, high $^{207}Pb/^{204}Pb_i$ and high $\delta^{18}O$; we suggest that this source reflects melting of low-Rb/Sr lower–crustal granulites associated with basaltic underplating of the crust. A subordinate crustal component (Crust 2) has low εNd_i, high $^{87}Sr/^{86}Sr_i$, moderate $^{207}Pb/^{204}Pb_i$ and high $\delta^{18}O$; we suggest that this source reflects melting of high Rb/Sr rocks at middle to upper crustal levels.

Lower crust (Crust 1). The consistent steep trend defined by the Antarctic Peninsula granitoids on εNd_i – $^{87}Sr/^{86}Sr_i$ plots cannot be generated by contamination of mantle-derived magmas by melts of exposed middle-upper crustal rocks. Although it is theoretically possible to approximate curves of the observed shape by AFC processes using a high-$^{87}Sr/^{86}Sr_i$ upper crustal end-member, the parameters required are geologically unreasonable. In addition, AFC curves can be highly sensitive to selected distribution coefficients and rates of assimilation: the consistent trends shown by the granitoid data would require similar AFC conditions to be maintained at various crustal levels throughout more than 200 Ma of magmatism. It is important to note that the composition of the low εNd_i, moderate $^{87}Sr/^{86}Sr_i$ crustal component appears to be rather uniform across the entire peninsula throughout it's magmatic history (Fig. 5), suggesting that it reflects melting of a widespread, isotopically homogeneous source.

Steep trends on εNd_i – $^{87}Sr/^{86}Sr_i$ plots may result from mixing with low Rb/Sr lower crustal material (DePaolo & Wasserburg 1979). For example, steep trends shown by granites from the North Patagonian batholith in southern Chile cannot be explained by mixing with melts derived from the accretionary complex into which the batholith was emplaced (Pankhurst *et al.* 1999). Rather, the granites are thought to have been derived by contamination of a mantle-derived magma with lower crust melts (Pankhurst *et al.* 1999).

An alternative view is given by Rogers & Hawkesworth (1989) for magmatic rocks of the northern Chilean Andes. These granitoids and volcanic rocks plot on two distinct trends on a plot of εNd_i against $^{87}Sr/^{86}Sr_i$, with a dog-leg distribution remarkably similar to that shown by the Antarctic Peninsula granitoids. Young volcanic rocks plot on a shallow trend between εNd_i values of –6 and –8, and $^{87}Sr/^{86}Sr_i$ values of 0.707 to 0.712, which Rogers & Hawkesworth (1989) ascribe to variable assimilation of crustal material. However, the majority of the data define a steep trend, between εNd_i values of +6 and –8, and values of 0.703–0.707. Rogers & Hawkesworth (1989) argue, on the basis of trace element modelling, that this steep trend is more likely to reflect mobilization of old mantle lithosphere, rather than contamination with lower crustal material.

The correlation of $\delta^{18}O$ and $^{87}Sr/^{86}Sr_i$ shown by Antarctic Peninsula granitoid data argues strongly for a component derived by anatexis and assimilation of lower crust material (Fig. 9). The steep trend defined by most of the data on Figure 9 suggests that the low-$^{87}Sr/^{86}Sr_i$ crustal end-member must have $\delta^{18}O > +9.5$. This value is higher than would be expected for primitive arc rocks, but falls well within the field defined by lower crustal xenoliths from the Ross Sea and Transantarctic Mountains, and is within error of average Transantarctic Mountains crust (Molzahn *et al.* 1996).

JOBNAME: JGS PAGE: 11 SESS: 33 OUTPUT: Wed Sep 26 15:06:45 2001
/hling/journals/geo/195/00139

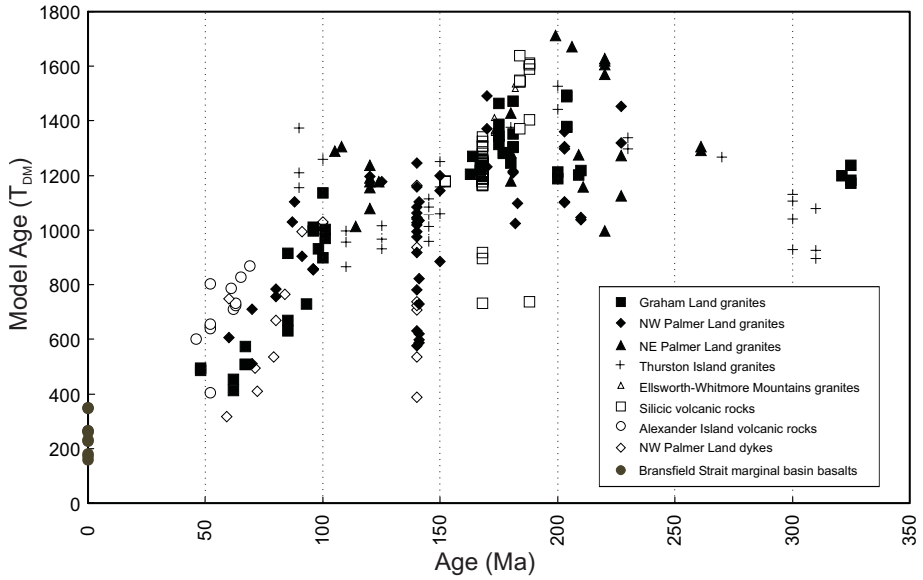

Fig. 10. Variation in T_{DM} through time. Granitoids and volcanic rocks of the Antarctic Peninsula, Ellsworth–Whitmore Mountains, and Thurston Island crustal blocks show similar overall trends, reflecting the changing geotectonic environment within West Antarctica through time. Additional data: Ellsworth–Whitmore Mountains granites, Pankhurst *et al.* (1991); Thurston Island, Pankhurst *et al.* (1991); Alexander Island, McCarron & Smellie (1998); silicic volcanic rocks, Pankhurst *et al.* (2000); NW Palmer Land dykes, Scarrow *et al.* (1998).

Upper crust (Crust 2). Assimilation of melts derived from high-$^{87}Sr/^{86}Sr_i$, high $\delta^{18}O$, low εNd_i middle to upper crustal rocks is of importance only in a few isolated Triassic to Mid-Jurassic granitoid bodies on the Antarctic Peninsula (Figs 5,8 & 9). In Graham Land, granitoids with a strong middle-upper crustal signature are restricted to a few square kilometres of Joerg Peninsula (Hole 1986; Fig. 2), and contain a large component derived by melting of local basement gneisses. In Palmer Land, such granitoids are restricted to the eastern part of the Peninsula, in the area around the Welch Mountains (Fig. 2). In this area, melting of basement paragneiss during Triassic to Early Jurassic magmatism has led to the lowest εNd_i and highest $^{87}Sr/^{86}Sr_i$ values shown by any Antarctic Peninsula granitoid (Wever *et al.* 1994).

Isotope signatures as an indicator of tectonic regime

A key feature of the observed trends between Sr, Nd, Pb and O isotopes in Figures 5, 8 and 9 is that samples fall either on a steep trend between mantle and lower crustal values, or on a shallow trend between lower and upper crustal reservoirs. Few samples plot between the trends, in a position which would be expected if mantle, lower crustal and upper crustal sources were involved in a single sample. This suggests that two distinct tectonic regimes were responsible for the observed trends. Samples that fall on shallow trends, with uniformly low εNd_i, high $\delta^{18}O$ and high, variable $^{87}Sr/^{86}Sr_i$, reflect mixing of a variety of crustal sources with little or no input from the mantle or from juvenile basaltic underplate. Such granitoids are restricted to Triassic to Mid-Jurassic times, and may have formed by melting entirely within the crust, in response to increased heat flow during lithospheric attenuation associated with the break-up of Gondwana. Samples which fall on steep trends on Figures 5, 8, and 9 are characterized by variable εNd_i, and relatively low $\delta^{18}O$ and $^{87}Sr/^{86}Sr_i$, reflecting interaction between mantle/juvenile underplate and lower crustal components. Such granitoids were emplaced intermittently throughout the history of magmatism along the Antarctic Peninsula, but are dominant from Early Cretaceous to Cenozoic times, and are thought to represent the products of normal subduction processes along the Antarctic Peninsula arc.

The granites of the Ellsworth–Whitmore Mountains plot on flat trends on plots of εNd_i and $\delta^{18}O$ against $^{87}Sr/^{86}Sr_i$. Correlation between their O- and Sr-isotope characteristics argues against involvement of the 'enriched' mantle component (Fig. 9) suggested by Storey *et al.* (1988). Rather, they are thought to result from mixing of crustal sources, as described above for the 'crust-dominated' Antarctic Peninsula granitoids.

Figure 10 summarizes the variation in depleted mantle Nd model age (T_{DM}) shown by granitoids and associated lithologies of the Antarctic Peninsula and adjacent crustal blocks of West Antarctica. T_{DM} gives a measure of the relative importance of crustal and mantle sources for a given sample; however, because the Nd-isotope characteristics of the proposed upper and lower crustal end-members are similar, these sources are not discriminated by T_{DM}.

Carboniferous and Permian granitoids from the Antarctic Peninsula and the adjacent Thurston Island crustal block (Fig. 1) have moderate T_{DM} (*c.* 900–1250), indicating that they contain a moderate proportion of the crustal component. In contrast, Triassic to Middle Jurassic granitoids emplaced before the initiation of rifting in the Weddell Sea show a considerable scatter in T_{DM}. Both 'normal' subduction-related and crust-dominated plutons were emplaced at this time, suggesting a complex interplay between tectonic processes. The highest T_{DM} values (>1300 Ma) are shown by plutons which have assimilated middle–upper crustal material. Following the initiation of Gondwana break-up the apparent role of crust diminishes, either reflecting a decrease in the degree of crustal melting within the arc, or caused by dilution of pre-Mesozoic crust by the addition of voluminous arc magmas. Granitoids from Graham Land and NE Palmer Land plot on smooth trends through Mesozoic times. A gap in the emplacement record in latest Jurassic–earliest Cretaceous times reflects compression within the arc associated with the Palmer Land deformation event (Storey *et al.* 1992, 1996). In contrast, the data from NW Palmer Land in earliest Cretaceous times show a major episode of pluton emplacement, with a wide range in Nd-isotope composition. This magmatism has been related to a major episode of extension within the arc (Vaughan & Millar 1996; Vaughan *et al.* 1997; Wareham *et al.* 1997*b*).

JOBNAME: JGS PAGE: 12 SESS: 33 OUTPUT: Wed Sep 26 15:06:45 2001
/hling/journals/geo/195/00139

Jurassic–Cretaceous granitoids of NE Palmer Land show similar variations of T_{DM} through time to granites from the adjacent Thurston Island crustal block (Pankhurst *et al*. 1993; Fig. 8). In particular, both NE Palmer Land and Thurston Island Cretaceous granitoids show a marked increase in T_{DM} at about 100 Ma. For the Thurston Island rocks, this increase has been ascribed to an increase of crustal anatexis associated with tectonic rearrangement of the west Gondwana margin, and initiation of active rifting between Marie Byrd Land and New Zealand. It is possible that the same process is reflected in the NE Palmer Land data.

Granitoids of Graham Land and NW Palmer Land show similar variations in T_{DM} with time between *c*. 120 and *c*. 50 Ma. It is notable that volcanic rocks on Alexander Island (Fig. 2) show distinctly higher T_{DM} for any given age during this period (Fig. 10), suggesting either that an older crustal component is involved, or that rates of crustal assimilation were systematically higher in Alexander Island at that time.

Conclusions

(1) Triassic to Cenozoic granitoids of the Antarctic Peninsula and the adjacent crustal blocks of West Antarctica show a wide range in Sr, Nd, and O isotope compositions, but a restricted range in Pb-isotope compositions.

(2) The majority of the granitoids are thought to have formed in response to subduction processes. Their isotopic characteristics can be explained by mixing of mafic arc magmas with melts derived from Proterozoic lower crust, in a process equivalent to the MASH model of arc magmatism proposed by Hildreth & Moorbath (1988). The mafic arc magmas are characterized by high εNd_i, low $^{87}Sr/^{86}Sr_i$, low $^{207}Pb/^{204}Pb_i$ and low $\delta^{18}O$, and may be derived from the mantle wedge (Leat *et al*. 1995), or by remelting of juvenile basaltic underplate (Wareham *et al.* 1997a). The mafic component is similar in isotopic composition to the Quaternary marginal-basin basalts of Bransfield Strait. The proposed lower crustal component is characterized by low εNd_i, moderate $^{87}Sr/^{86}Sr_i$, high $^{207}Pb/^{204}Pb_i$ and high $\delta^{18}O$.

(3) The subduction-related granitoids show consistent trends of increasing εNd_i, and decreasing $^{87}Sr/^{86}Sr_i$, $^{207}Pb/^{204}Pb_i$, and $\delta^{18}O$ through time. This might reflect a decrease in the degree of crustal melting with time, but more probably reflects dilution of the Proterozoic lower crustal component with voluminous arc magmas emplaced throughout the Mesozoic. The restricted range in Pb-isotope composition shown by the granitoids may reflect homogenization of Pb in the crust within deep, large-scale, fluid advection systems (McCulloch & Woodhead 1993).

(4) In contrast to the arc-derived granitoids, many Triassic to Mid-Jurassic granitoid suites have uniformly low εNd_i, high $\delta^{18}O$, and variable $^{87}Sr/^{86}Sr_i$, and are best explained by mixing of melts derived from lower (low-$^{87}Sr/^{86}Sr$) and middle (high-$^{87}Sr/^{86}Sr$) crust with little or no contribution from mantle-derived magmas. These granitoids are thought to have formed in an intra-plate setting, in response to crustal extension preceding and accompanying the break-up of Gondwana. In NE Palmer Land, emplacement of such intra-plate granites alternated with emplacement of subduction-related granitoids throughout Triassic–Middle Jurassic times. The initiation of subduction along the palaeo-Pacific margin of Gondwana in Triassic times appears to have coincided with a phase of intermittent extension within the continent, which continued until continental break-up took place in the Jurassic.

(5) Correlations between Sr and O isotopes demonstrate that melting of an enriched Ferrar/Karoo-type lithospheric mantle is not involved in the genesis of granitoids of the Antarctic Peninsula or of the Ellsworth–Whitmore Mountains crustal block.

Thanks are due to the many geologists of the British Antarctic Survey, past and present, whose data are synthesized in this paper. We would like to thank M. Hole, P. Leat, A. Milne, R. Pankhurst, and A. Vaughan for many useful discussions and comments. We are particularly grateful to W. Hildreth and A. Saunders for their constructive and helpful reviews.

References

Atherton, M.P. & Petford, N. 1993. The generation of sodium-rich magmas from newly underplated basaltic crust. *Nature*, **362**, 144–146.

Barker, P.F. 1982. The Cenozoic subduction history of the Antarctic Peninsula: ridge crest–trench interactions. *Journal of the Geological Society, London*, **139**, 787–801.

Clayton, R.N. & Mayeda, T.K. 1963. The use of bromine pentafluoride in the extraction of oxygen from oxides and silicates for oxygen isotope analysis. *Geochimica et Cosmochimica Acta*, **27**, 43–52.

Defant, M.J. & Drummond, M.S. 1990. Derivation of some modern arc magmas by melting of young subducted lithosphere. *Nature*, **347**, 662–665.

DePaolo, D.J. 1981. Trace element and isotopic effects of combined wall-rock assimilation and fractional crystallisation. *Earth and Planetary Science Letters*, **53**, 189–202.

DePaolo, D.J. & Wasserburg, G.J. 1979. Petrogenetic mixing models and Nd-Sr isotopic patterns. *Geochimica et Cosmochimica Acta*, **43**, 615–627.

DePaolo, D.J., Linn, A.M. & Schubert, G. 1991. The continental crustal age distribution–methods of determining mantle separation ages from Sm-Nd isotopic data and application to the south-western United States. *Journal of Geophysical Research*, **96**, 2071–2088

Gariépy, C. & Allègre, C.J. 1985. The lead isotope geochemistry and geochronology of late-kinematic intrusives from the Abitibi greenstone belt, and implications for Late Archean crustal evolution. *Geochimica et Cosmochimica Acta*, **49/11**, 2371–2383.

Gradstein, F.M. & Ogg, J. 1996. A Phanerozoic time scale. *Episodes*, **19**.

Harris, C., Marsh, J.S., Duncan, A.R. & Erlank, A.J. 1990. The petrogenesis of the Kirwan basalts of Dronning Maud Land, Antarctica. *Journal of Petrology*, **31**, 341–369.

Harrison, S.M. & Piercy, B.A. 1991. Basement gneisses in north-west Palmer Land: further evidence for pre-Mesozoic rocks in Lesser Antarctica. *In:* Thomson, M.R.A., Crame, J.A. & Thomson, J.W. (eds) *Geological Evolution of Antarctica*. Cambridge University Press, Cambridge, 341–344.

Hildreth, W. & Moorbath, S. 1988. Crustal contributions to arc magmatism in the Andes of Central Chile. *Contributions to Mineralogy and Petrology*, **98**, 455–489.

Hole, M.J. 1986. *Time controlled geochemistry of igneous rocks of the Antarctic Peninsula*. PhD Thesis, University of London.

Hole, M.J., Pankhurst, R.J. & Saunders, A.J. 1991 Geochemical evolution of the Antarctic Peninsula magmatic arc: the importance of mantle-crust interactions during granitoid genesis. *In:* Thomson, M.R.A., Crame, J.A. & Thomson, J.W. (eds). *Geological Evolution of Antarctica*. Cambridge University Press, Cambridge, 369–374.

James, D.E. 1981. The combined use of oxygen and radiogenic isotopes as indicators of crustal contamination. *Annual Review of Earth and Planetary Sciences*, **9**, 311–344.

Keller, R.A., Fisk, M.R., White, W.M. & Birkenmajer, K. 1991. Isotopic and trace element constraints on mixing and melting models of marginal basin volcanism, Bransfield Strait, Antarctica. *Earth and Planetary Science Letters*, **111**, 287–303.

Kempton, P.D. & Harmon, R.S. 1992. Oxygen isotope evidence for large-scale hybridisation of the lower crust during magmatic underplating. *Geochimica et Cosmochimica Acta*, **56**, 971–986.

Kempton, P.D., Downes, H. & Embey-Isztin, A. 1997. Mafic granulite xenoliths in Neogene alkali basalts from the western Pannonian Basin: insights into the lower crust of a collapsed orogen. *Journal of Petrology*, 7 **38**, 941–970.

Kyle, P.R., Pankhurst, R.J. & Bowman, J.R. 1983. Isotopic and chemical variations in Kirkpatrick basalt group rocks from southern Victoria Land. *In:* Oliver, R.L., James, P.R. & Jago, J.B. (eds) *Antarctic Earth Science*. Australian Academy of Science, 234–237.

Larter, R.D. & Barker, P.F. 1991. Effects of ridge crest-trench interaction on Antarctic-Phoenix spreading: forces on a young subducting plate. *Journal of Geophysical Research*, **96**, 19583–19607.

Leat, P.T., Scarrow, J.H. & Millar, I.L. 1995. On the Antarctic Peninsula Batholith. *Geological Magazine*, **132**, 399–412.

Loske, W. & Miller, H. 1991. Rb–Sr and U–pb geochronology of basement xenoliths at Cape Dubouzet, Antarctic Peninsula. *In: 6th International Symposium on Antarctic Earth Sciences, Abstracts*, 374–379.

McCarron, J.J. & Smellie, J.L. 1998. Tectonic implications of fore-arc magmatism and generation of high-magnesian andesites: Alexander Island, Antarctica. *Journal of the Geological Society, London*, **155**, 269–280.

McCulloch, M.T. & Woodhead, J.D. 1993. Lead isotope evidence for deep crustal-scale fluid transport during granite petrogenesis. *Geochimica et Cosmochimica Acta*, **57**, 659–674.

Millar, I.L. & Pankhurst, R.J. 1987. Rb–Sr geochronology of the region between the Antarctic Peninsula and the Transantarctic Mountains: Haag Nunataks and Mesozoic granitoids. *In:* McKenzie, G.D. (ed.) *Gondwana Six: Structure, Tectonics and Geophysics*. American Geophysical Union, Geophysical Monographs, **40**, 151–160.

Millar, I.L., Pankhurst, R.J. & Fanning, C.M. in press. Basement chronology of the Antarctic Peninsula: recurrent magmatism and anatexis in the Palaeozoic Gondwana margin. *Journal of the Geological Society, London*.

Milne, A.J. 1990. *The pre-Mesozoic geological evolution of Graham Land, Antarctica*. PhD Thesis, Open University.

Milne, A.J. & Millar, I.L. 1989. The significance of mid-Palaeozoic basement in Graham Land, Antarctic Peninsula. *Journal of the Geological Society, London*, **146**, 207–210.

Molzahn, M., Reisberg, L. & Wörner, G. 1996. Os, Sr, Nd, Pb, O isotope and trace element data from the Ferrar flood basalts, Antarctica: evidence for an enriched subcontinental lithospheric source. *Earth and Planetary Science Letters*, **144**, 529–546.

Pankhurst, R.J. 1982. Rb-Sr geochronology of Graham Land, Antarctica. *Journal of the Geological Society, London*, **139**, 701–711.

Pankhurst, R.J. 1983. Rb-Sr constraints on the ages of basement rocks of the Antarctic Peninsula. *In:* Oliver, R.L., James, P.R. & Jago, J.B. (eds) *Antarctic Earth Science*. Australian Academy of Science, 367–371.

Pankhurst, R.J. 1990. The Palaeozoic and Andean magmatic arcs of West Antarctica and southern South America. *In:* Kay, S.M. & Rapela, W.W. (eds) *Plutonism from Antarctica to Alaska*. Geological Society of America Special Papers, **241**, 1–8.

Pankhurst, R.J. & Rapela, C.R. 1995. Production of Jurassic rhyolite by anatexis of the lower crust of Patagonia. *Earth and Planetary Science Letters*, **134**, 23–36.

Pankhurst, R.J., Hole, M.J. & Brook, M. 1988. Isotope evidence for the origin of Andean granites. *Transactions of the Royal Society of Edinburgh: Earth Sciences*, **79**, 123–133.

Pankhurst, R.J., Storey, B.C. & Millar, I.L. 1991. Magmatism related to the break-up of Gondwanaland. *In:* Thomson, M.R.A., Crame, J.A. & Thomson, J.W. (eds) *Geological Evolution of Antarctica*. Cambridge University Press, Cambridge, 573–579.

Pankhurst, R.J., Millar, I.L., Grunow, A.M. & Storey, B.C. 1993. The pre-Cenozoic magmatic history of the Thurston Island crustal block, West Antarctica. *Journal of Geophysical Research*, **98**, 11835–11849.

Pankhurst, R.J., Weaver, S.D., Hervé, F. & Larrondo, P. 1999. Mesozoic-Cenozoic evolution of the North Patagonian batholith in Aysén, southern Chile. *Journal of the Geological Society, London*, **156**, 673–694.

Pankhurst, R.J., Riley, T.R., Fanning, C.M. & Kelley, S.P. 2000. Episodic silicic volcanism in Patagonia and the Antarctic Peninsula: Chronology of magmatism associated with the break-up of Gondwana. *Journal of Petrology*, **41**, 605–625.

Rogers, G. & Hawkesworth, C.J. 1989. A geochemical traverse across the North Chilean Andes: evidence for crust generation from the mantle wedge. *Earth and Planetary Science Letters*, **91**, 271–285.

Saunders, A.D., Tarney, J. & Weaver, S.D. 1980. Transverse geochemical variations across the Antarctic Peninsula: implications for the genesis of calc-alkaline magmas. *Earth and Planetary Science Letters*, **46**, 344–360.

Scarrow, J.H., Pankhurst, R.J., Leat, P.T. & Vaughan, A.P.M. 1996. Antarctic Peninsula granitoid petrogenesis: a case study from Mount Charity, north-eastern Palmer Land. *Antarctic Science*, **8**, 193–206.

Scarrow, J.H., Leat, P.T., Wareham, C.D. & Millar, I.L. 1998. Geochemistry of mafic dykes in the Antarctic Peninsula continental-margin batholith: a record of arc evolution. *Contributions to Mineralogy and Petrology*, **132**, 208–208.

Storey, B.C. & Alabaster, T. 1991. Tectonomagmatic controls on Gondwana break-up models: evidence from the proto-Pacific margin of Antarctica. *Tectonics*, **10**, 1274–1288.

Storey, B.C., Hole, M.J., Pankhurst, R.J., Millar, I.L. & Vennum, W. 1988. Middle Jurassic within-plate granites in West Antarctica and their bearing on the break-up of Gondwana. *Journal of the Geological Society, London*, **145**, 999–1007.

Storey, B.C., Grunow, A.M., Dalziel, I.D.W., Pankhurst, R.J. & Millar, I.L. 1991. A new look at the geology of Thurston Island. *In:* Thomson, M.R.A., Crame, J.A. & Thomson, J.W. (eds) *Geological Evolution of Antarctica*. Cambridge University Press, Cambridge, 399–403.

Storey, B.C., Alabaster, T., Hole, M.J., Pankhurst, R.J. & Wever, H.E.1992. Role f subduction-plate boundary forcs during the initial stages of Gondwana break-up: evidence for the proto-Pacific margin of Antarctica. *In:* Storey, B.C., Alabaster, T. & Pankhurst, R.J. (eds) *Magmatism and the Causes of Continental Break-up*. Geological Society, London, Special Publications, **68**, 149–164.

Storey, B.C., Vaughan, A.P.M. & Millar, I.L. 1996. Geodynamic evolution of the Antarctic Peninsula during Mesozoic times and its bearing on Weddell Sea history. *In:* Storey, B.C., King, E.C. & Livermore, R.A. (eds) *Weddell Sea Tectonics and Gondwana Break-up*. Geological Society, London, Special Publications, **108**, 87–103.

Suarez, M. 1976. Plate tectonic model for southern Antarctic Peninsula and its relation to southern Andes. *Geology*, **4**, 211–214.

Sultan, M., Bickford, M.E., Kaliouby, B.El. & Arvidson, R.E. 1992. Common Pb systematics of Precambrian granitic rocks of the Nubian Shield (Egypt) and tectonic implications. *Geological Society of America Bulletin*, **104**, 456–470

Tangeman, J.A., Mukasa, S.B. & Grunow, A.M. 1996. Zircon U-Pb geochronology of plutonic rocks from the Antarctic Peninsula: confirmation of the presence of unexposed Paleozoic crust. *Tectonics*, **15**, 1309–1324.

Taylor, S.R. & McLennan, S.M. 1995. The geochemical evolution of the continental crust. *Reviews of Geophysics*, **33**, 241–265.

Todt, W., Cliff, R.A., Hanser, A. & Hoffmann, A.W. 1984. $^{202}Pb + {}^{205}Pb$ double spike for lead isotope analysis. *Terra Cognita*, **4**, 209

Vaughan, A.P.M. & Millar, I.L. 1996. Early Cretaceous magmatism during extensional deformation within the Antarctic Peninsula magmatic arc. *Journal of South American Earth Sciences*, **9**, 121–129.

Vaughan, A.P.M. & Storey, B.C. 2000. Terrane accretion and collision: a new tectonic model for the Mesozoic development of the Antarctic Peninsula magmatic arc. *Journal of the Geological Society*, **157**, 1243–1256.

Vaughan, A.P.M., Wareham, C.D. & Millar, I.L. 1997. Granitoid pluton formation by spreading of continental crust: the Wiley Glacier complex, northwest Palmer Land, Antarctica. *Tectonophysics*, **283**, 35–60.

Wareham, C.D., Millar, I.L. & Vaughan, A.P.M. 1997a. The generation of sodic granite magmas, western Palmer Land, Antarctic Peninsula. *Contributions to Mineralogy and Petrology*, **128**, 81–96.

Wareham, C.D., Vaughan, A.P.M. & Millar, I.L. 1997b. The Wiley Glacier complex, Antarctic Peninsula: pluton growth by pulsing of granitoid magmas. *Chemical Geology*, **143**, 65–80.

Wever, H.E. & Storey, B.C. 1992. Bimodal magmatism in northeast palmer Land, Antarctic Peninsula: geochemical evidence for a Jurassic ensialic back-arc basin. *Tectonophysics*, **205**, 239–259.

Wever, H.E., Millar, I.L. & Pankhurst, R.J. 1994. Geochronology and radiogenic isotope geology of Mesozoic rocks from eastern Palmer Land, Antarctic Peninsula: crustal anatexis in arc-related granitoid genesis. *Journal of South American Earth Sciences*, **7**, 69–83.

Wever, H.E., Storey, B.C. & Leat, P.T. 1995. Peraluminous granites in NE Palmer Land, Antarctic Peninsula: early Mesozoic crustal melting in a magmatic arc. *Journal of the Geological Society, London*, **152**, 85–96.

Willan, R.C.R. & Swainbank, I.G. 1995. Galena lead isotopic variations in a Mesozoic-Cenozoic Andean arc, Antarctic Peninsula. *Journal of the Geological Society, London*, **152**, 767–778.

Received 21 September 2000; revised typescript accepted 16 May 2001.
Scientific editing by Sally Gibson.